IRANIAN JOURNAL OF PHYSICS RESEARCH

Iranian Journal of Physics Research, Vol. 16, No. 3, 2016

Effect of annealing temperature on optical and electrochromic properties of tungsten oxide thin films

A Abareshi and H Haratizadeh

Department of Physics, Shahrood University of Technology, Shahrood, Iran

E-mail: hamha@shahrovdut.ac.ir

(Received 3 December 2014 ; in final form 25 February 2016)

Abstract

Tungsten trioxide (WO_3) thin films were coated onto fluorine tin oxide coated glass substrates, using electrodeposition technique via aqueous solution of peroxotungstic acid. WO_3 films were evaluated as a function of annealing temperature (60°C, 100°C, 250°C and 400°C). The films were analyzed by field emission Scanning Electron Microscopy (SEM), UV-visible spectrometer and cyclic voltammogram. The films had high transmission in optical visible region. Using optical transmittance and cyclic voltammogram measurements, the electrochromic properties of WO_3 films were investigated in a non-aqueous lithium perchlorate in propylene carbonate electrolyte. Increasing the annealing temperature will decrease electrochromic and optical properties of WO_3 films, since it leads to increasing the size of grains. Therefore, having been annealed at 60°C, WO_3 film exhibited a noticeable electrochromic performance with a high transmission modulation and Coloration Efficiency Efficiency (CE) of 64.1 $cm^2\ C^{-1}$ at wavelength equal to 638 nm.

Keywords: tungsten oxide, electrochromic, electrodeposition, cyclic voltammogram

1. Introduction

Electrochromic materials are able to change their optical properties reversibly and persistently by an external voltage[1]. Theses materials have attracted substantial scientific and industrial attention because of their optical modulation in visible or infrared regions. There has been a great interest in electrochromic applications and fabrication devices such as architectural applications including energy efficient glazing, privacy glass, partitions and skylights [2].

Transition metal oxide thin films such as oxides of W, V, Ir, Ti and Ni have been widely studied for their electrochromic behavior [1]. Among these materials, WO_3 is considerably interesting due to its high Coloration Efficiency (CE), good cycle reversibility, long life and low material cost [3-6]. As a typical electrochromic material, WO_3 has been widely investigated because of its potential applications in information displays [3], energy-saving smart windows [5-8], variable-emittance thermal radiators [9] and variable-reflectance mirrors [10].

In WO_3 thin films, electrochromic property is achieved when Li^+ ions are inserted into these films, since the valance state of W^{6+} changes to a W^{6+}/ W^{5+} mixed state [11]. Therefore, to achieve a fast and sufficient intercalation of ions, high surface ratio of EC films such as nano-structured or porous films is required [12, 13].

Nanostructured WO_3 films have been synthesized using several methods such as sol–gel [14], electrodeposition [15-18], template method [17], anodic oxidation [18], chemical vapor deposition [19], electro spinning [20], electron beam evaporation [21], hydrothermal oxidation [22], atmospheric pressure plasma jet [23], etc.

In this research, electrodeposition method was employed to prepare highly porous WO_3 films. This aimed at comparing electrochromic properties of electrodeposited WO_3 films as a function of annealing temperature, investigating the morphology of these films as well as their optical and electrochemical properties. In this study, the effect of annealing temperature on electrochromic properties of Glass/ fluorine Thin Oxide (FTO) / WO_3 was determined by cyclic voltammogram in constant voltage. Coated layers were characterized by electrochemical and transmittance measurement in order to evaluate their electrochromic performance levels. The surfaces of the films were also

studied by Scanning Electron Microscopy (SEM). The results demonstrated that the films which were prepared after annealing at 60°C, exhibited improved ion mobility in comparison with films annealed in high temperatures; and the highest values of Coloration Efficiency (CE) were observed after annealing at 60°C.

2. Experimental details

2.1. Preparation of peroxotungstic solution

To prepare peroxotungstic acid solution, 3.25 g of tungsten metal powder (99% pure) was dissolved in 20 ml 30% H_2O_2 (Qualigens) and 2 ml distilled water. Addition of W powder into H_2O_2 was conducted in a chilled water bath under continuous agitation because peroxotungstic acid formation is a strong exothermic reaction. Then, the tungsten-peroxide solution should be kept in a refrigerator at about 2 °C.

To be completely dissolved, all W should be kept at such low temperatures for about a week. The result is a colorless solution of peroxotungstic acid. However, this solution still contains an excess quantity of H_2O_2 which leads to parasitic reactions and impedes an efficient electrodeposition. More than 8 days of low temperature (2 °C) is required to dispose it. Gradual reduction of peroxide at low temperatures was more preferable than other less time-consuming methods such as treatment with tungsten bronze, as it prevents precipitation of WO_3 sediment (yellow powder). Peroxotungstic acid colloidal solution which is obtained by this procedure can be kept at 2 °C for a few weeks [16].

2.2. Deposition of WO_3 thin film

20 ml of the above solution was mixed with 20 ml anhydrous ethanol at room temperature under continuous agitation. It yielded a bright yellow liquid. The liquid was heated to 60°C for 30 min before deposition. This solution will remain stable for a maximum of 10 days if it is preserved at temperatures below 10°C.

The films were deposited under potentiostatic conditions in a three-electrode electrochemical cell with a 2.5×2.5 cm^2 fluorine-doped tin oxide (SnO_2:F) coated glass substrate as the working electrode, a Saturated Calomel Electrode (SCE) as the reference electrode and a platinum sheet being the counter electrode. The working electrode was subjected to a constant cathodic potential of -493 mV for 10 min at room temperature. The films looked deep blue during the preparation process. This signifies a reduced oxidation state for tungsten. Having removed the films from the solution, this color vanishes immediately. The films were then sunk in deionized water. The coated samples were dried and then annealed at different temperatures (60°C, 100°C, 250°C and 400°C) for 90 min. This process yields high quality WO_3 films with an acceptable degree adherence to the substrate.

2.3. Instrumentation and experimental techniques

The surface morphology was observed by field emission scanning electron microscopy (FESEM; Hitachi S-4160). The thickness of the films was measured by Taly profile Gold / Hobson 5.1.1.5374. Transmission spectra were recorded for colored and bleached films in 300-1100 nm wavelength range with respect to air in the reference beam in UV-1800 PC Shimadzu spectrophotometer. Cyclic voltammogram for the films was performed in a three-electrode electrochemical cell between -1.5 and +1.5 V, where a WO_3 film was deposited on SnO_2: F coated glass substrate acted as the working electrode. SCE was also used as the reference electrode and Pt foil was employed as the auxiliary. The measurements were performed in an electrolyte solution of lithium perchlorate in propylene carbonate with 1M density (1M $LiClO_4$-PC) with scan rates of 50 mv/s (BEHPAJOOH , BHP2063+).

3. Results and discussion

3.1. Surface morphology of the films

Figure 1 shows SEM micrographs of the surfaces of films that were deposited with different annealing temperatures (60°C, 100°C, 250°C and 400°C). The surfaces of films are fairly uniform with only a few large aggregates of WO_3 particles. As can be seen in figure1,these aggregates affect the existing films by creating cracks on their surface. The microstructures reveal a glazy contrast through the films and a distinction between grains. It is observed that by increasing the annealing temperature, gradual increment in the grain size will occur. Therefore, the film which is annealed at 60°C, has a more open structure in contrast to the films which are annealed at higher temperatures.

3.2. Optical properties of the films

Figure 2 illustrates the optical transmittance spectra within $300 \leq \lambda \leq 1100$ nm wavelength range for WO_3 films with different annealing temperatures at the 9^{th} cycle, in colored and bleached states. The color of the WO_3 film changes from blue (colored state), to near transparent (bleached state), by applying step potential of -1.4 V to +1.4 V (vs. SCE). Transmittance modulation is about 65.9% for the film which is annealed at 60°C and it is significantly lower for the film which is annealed at 100°C ($\Delta T = 32.3$ %). This amount increases again upon future annealing to acquire values of 46.43 % and 38.75% for 250°C and 400°C films respectively.

In order to explore the optical properties in more details, the result of figure 2a is quantified in figure 2b. Figure 2b shows the transmission modulation as a function of annealing temperature. It reveals that maximum transmission modulation is obtained for WO_3 film that is annealed at 60°C, because it is generally believed that high porous structure will allow better penetration of electrolyte to promote lithium ions diffusion. During electrode reaction, the diffusion length of lithium ions in the film is short, resulting in fact insertion /extraction reaction and thus obtaining good performance [7]. This implies that WO_3 film annealed at 60°C has good electrochromic properties. This value is higher than the reported ΔT values for WO_3 films that were deposited by wet chemical techniques [24,25]. High transmittance($55\% \leq T \leq 74.5\%$) is retained by bleached film in the entire visible range. Integrated visible transmittance of the film annealed at 60 °C is

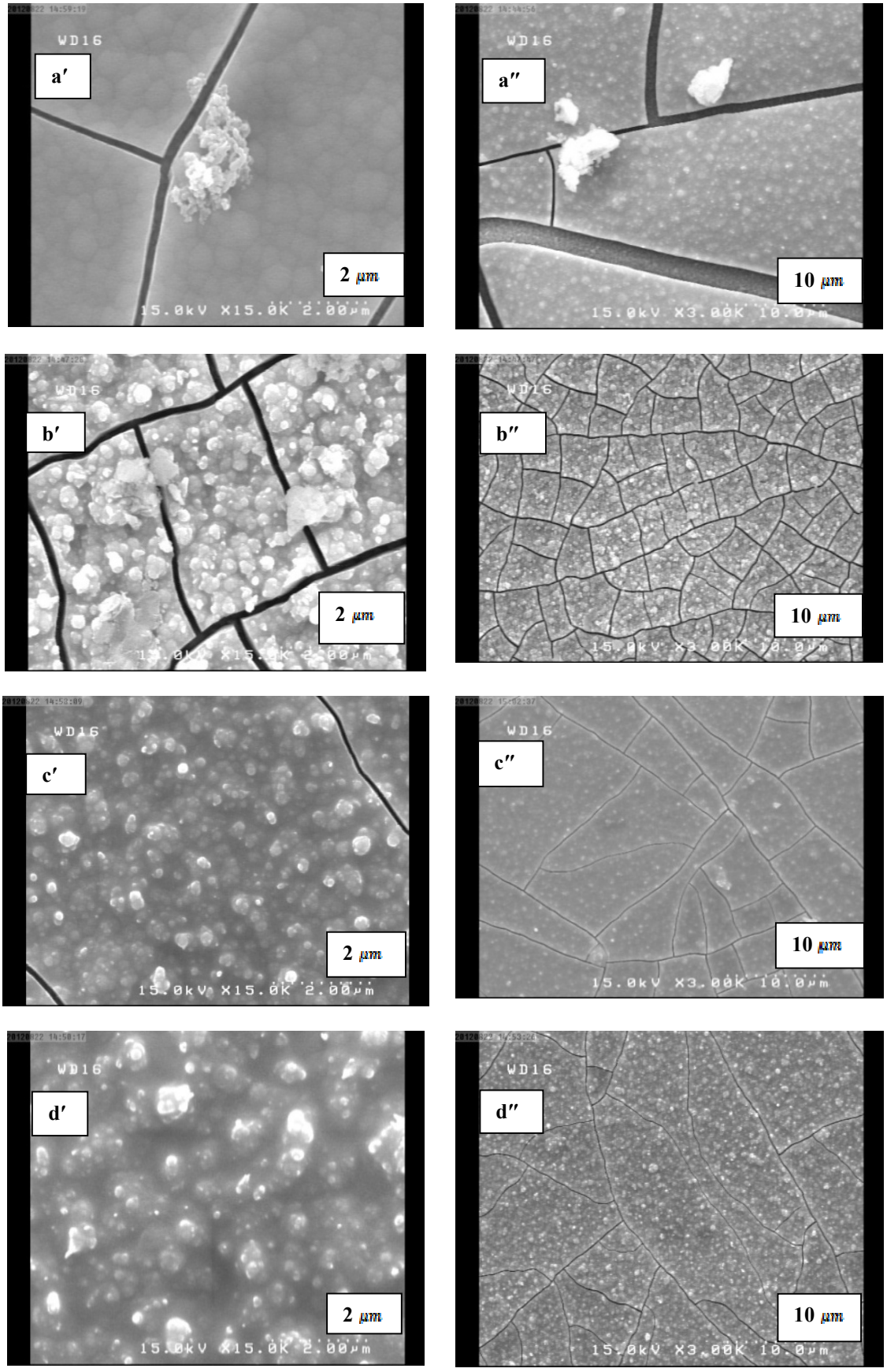

Figure. 1. SEM image of WO_3 films annealed at 60°C (a′, a″), 100°C (b′,b″), 250°C (c′, c″), and 400°C (d′, d″).

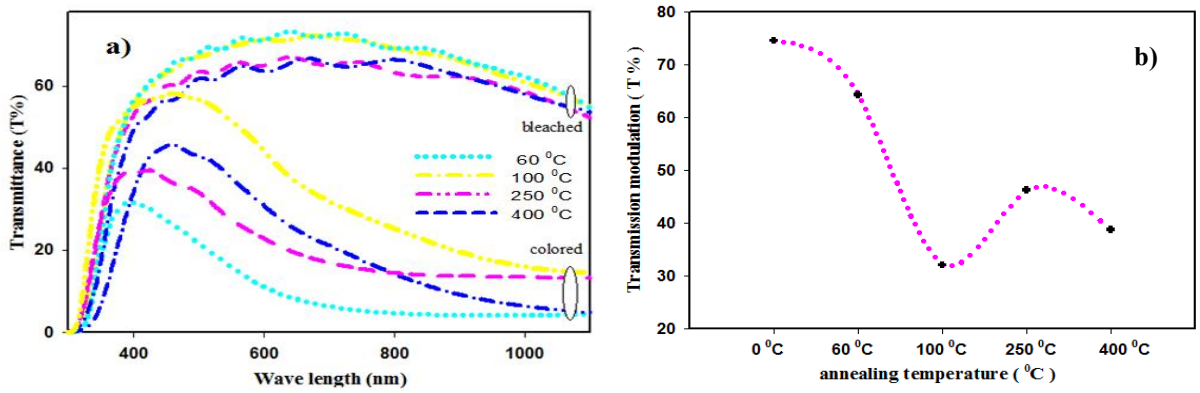

Figure 2. (a) Optical transmittance spectra of WO_3 thin films annealed at different temperatures in colored and bleached states within $300 \leq \lambda \leq 1100$ nm range, (b) transmission modulation as a function of annealing temperature, as calculated from data in figure 3a.

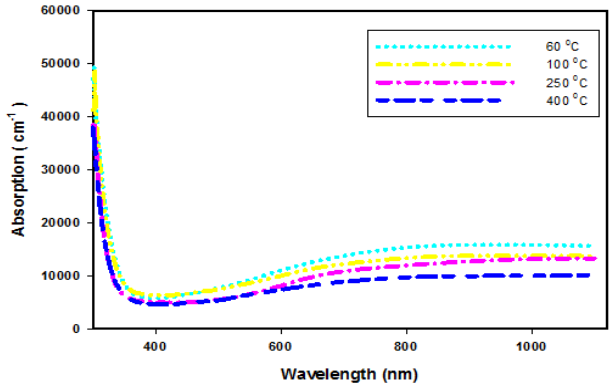

Figure 3. Absorptance spectra of WO_3 films annealed at 60°C, 100°C, 250 °C and 400 °C in colored state.

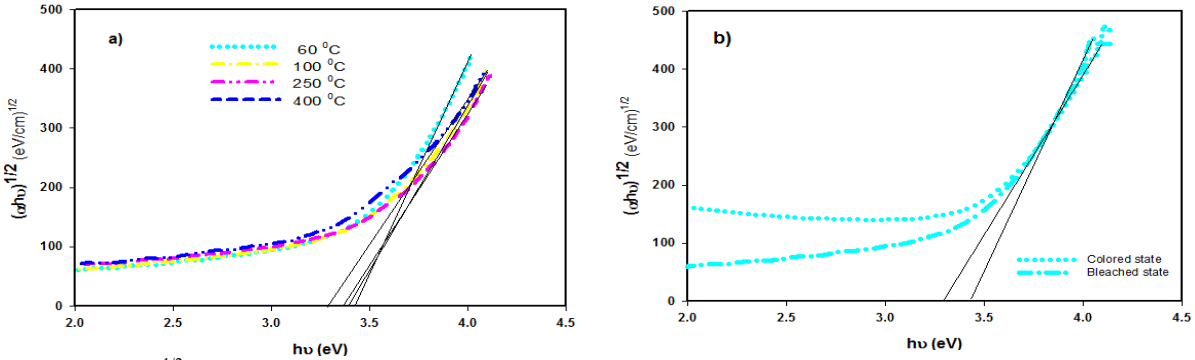

Figure 4. Plot $(\alpha h\nu)^{1/2}$ vs. $(h\nu)$ for WO_3 films annealed at (a) different temperatures in bleached state, (b) 60°C in colored and bleached states.

~74.5% and it drops to ~55% in solar region due to an increase in reflectance from underlying SnO_2: F substrate Near Infrared Region (NIR). This is more than sufficient for its use in electrochromic windows.

Electrochemical measurments on WO_3 spin-coated films of a peroxotungstic ester complex in ethanol exhibited a ΔT_{vis} = 60% [26]. A transmission modulation of ~40 to 50% in the visible range was observed for a WO_3 film deposited from a poly tungstic acid sol and cured at 250-300°C by Biswas et al. [27]. Shiyanovskaya et al. [28], found a ΔT_{vis} = 46% for a WO_3 film comprising polymorphic hexagonal form of WO_3 nanocrystallites.

In figure 3 absorbance spectra appears for coloration of WO_3 films which are annealed at 60°C, 100°C, 250 °C and 400 °C. It should be noted that the appearing spectra in figure 3 was calculated from eq. (1)

$$\alpha = (-1/t)\,LnT, \qquad (1)$$

where α is the absorption coefficient, t and T are thickness and amount of transmission respectively. Surface profiles of these films were investigated by a Talyprofile and the results showed that films appear to be 1.70-1.76 μm thick. Figure 3 shows that the increased size of grains does not impede the optical properties of WO_3 film. Indeed, in the bleached state, WO_3 film that is annealed at 60 °C, appears to be significantly transparent (T ≈ 74.5 % at 663 nm). As it becomes progressively colored (T ≈ 8.6%, A ≈ 13405.7 cm-1 at 663 nm), an increase in absorbance can be observed. This fact confirms the absorption-oriented nature of the device coloration, which is compatible with the observation of others for amorphous films [16].

Figure 4. shows plot of $(\alpha h\nu)^{1/2}$ as a function of

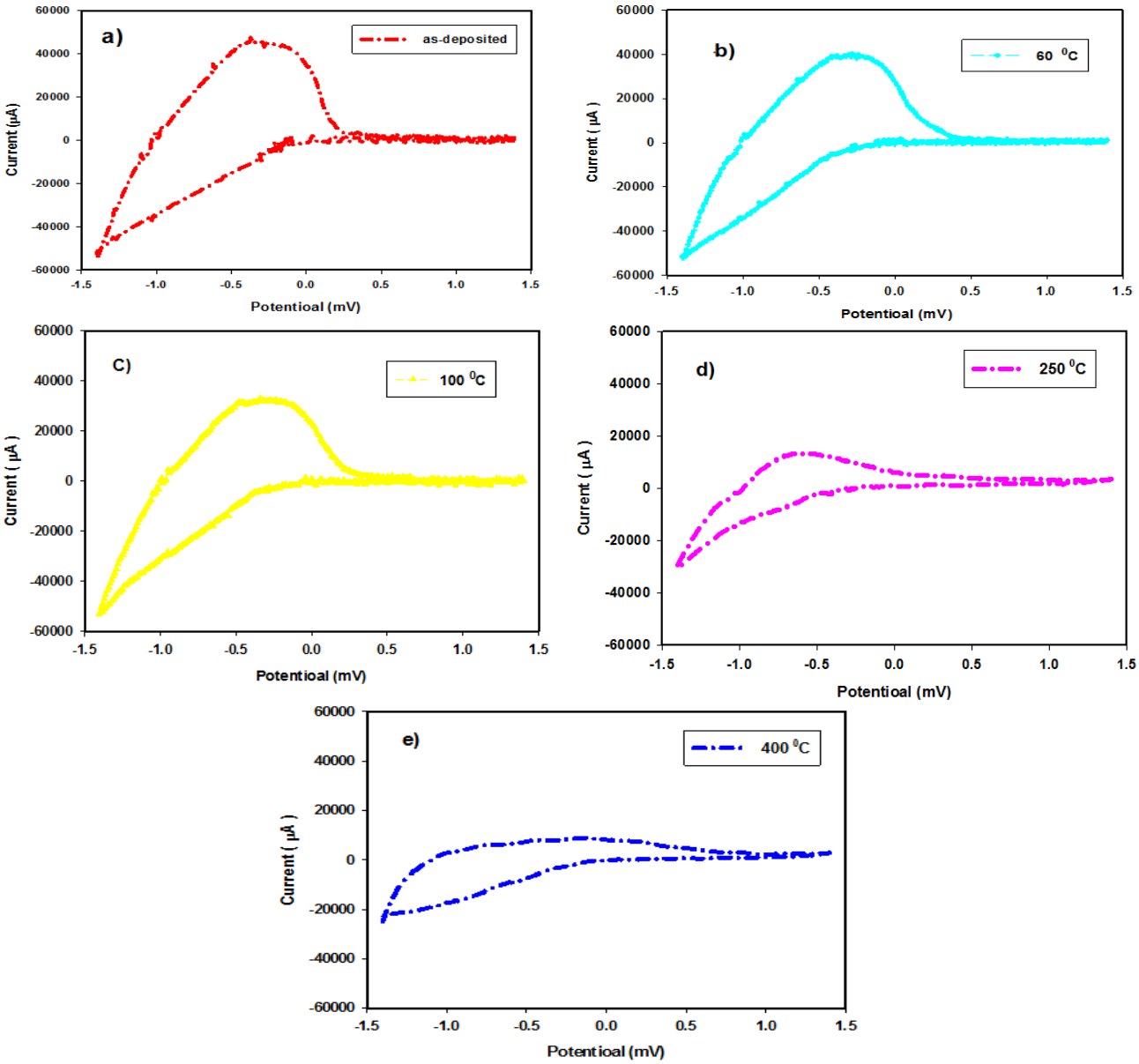

Figure 5. Cyclic voltammograms for films annealed at (a) as-deposited, (b) 60°C, (c)100°C, (d) 250 °C and (e) 400 °C recorded at 50 mV s^{-1} in a 1 M $LiClO_4$-PC electrolyte.

photon energy ($h\nu$) for WO_3 thin films deposited on FTO–coated glass substrates as a function of film annealing temperature.Using eq. (2) is allowed for direct transitions [29]. The optical band gap (E_g) of WO_3films was calculated in the bleached.

$$(\alpha h\nu)^{1/2} = A(h\nu - E_g), \quad (2)$$

where α is the absorption coefficient, hν is the photon energy and A is the constant. The results are shown in. figure 4a. Linear extrapolations led to an estimate of the optical band gaps values. It is observed that, as the annealing temperature increases, gradual decrement will take place in band gap energy of the films from 3.4 eV to 3.31 eV for bleached state. The E_g in the colored state is lower than the one in the bleached state (Figure 4b). It has been reported that the band gap of WO_3 powder is about 3.25 eV [30]. Deepa et al. [31] also reported colored WO_3 film with the band gap of 2.60 eV. Yang et al. [29] also reported colored WO_3 film with the band gap of 3.25 eV. The results in this study are in good agreement with their research.

3.3. Electrochromic performance of films

Electrochromic characteristic is the most important property of EC materials. The Cyclic Voltammogram (CV) plots of five electrodeposited WO_3 films with different annealing temperatures are compared in figure 5. All data presented here were obtained with the same sweep rate of 50 mV/s after 9 consecutive coloration-bleaching cycles using 1 M $LiClO_4$-PC. Typical broad featureless peaks show Li^+ insertion/extraction in WO_3 films.The position of ill-defined anodic peak current shifts to more negative potentials with increasing annealing temperature and respective of the annealing temperature, the value of the maximum current decreases with increasing annealing temperature.The coloration current, an indicator of the speed of Li^+ insertion into films, is higher at the lowest negative value on CV plots.

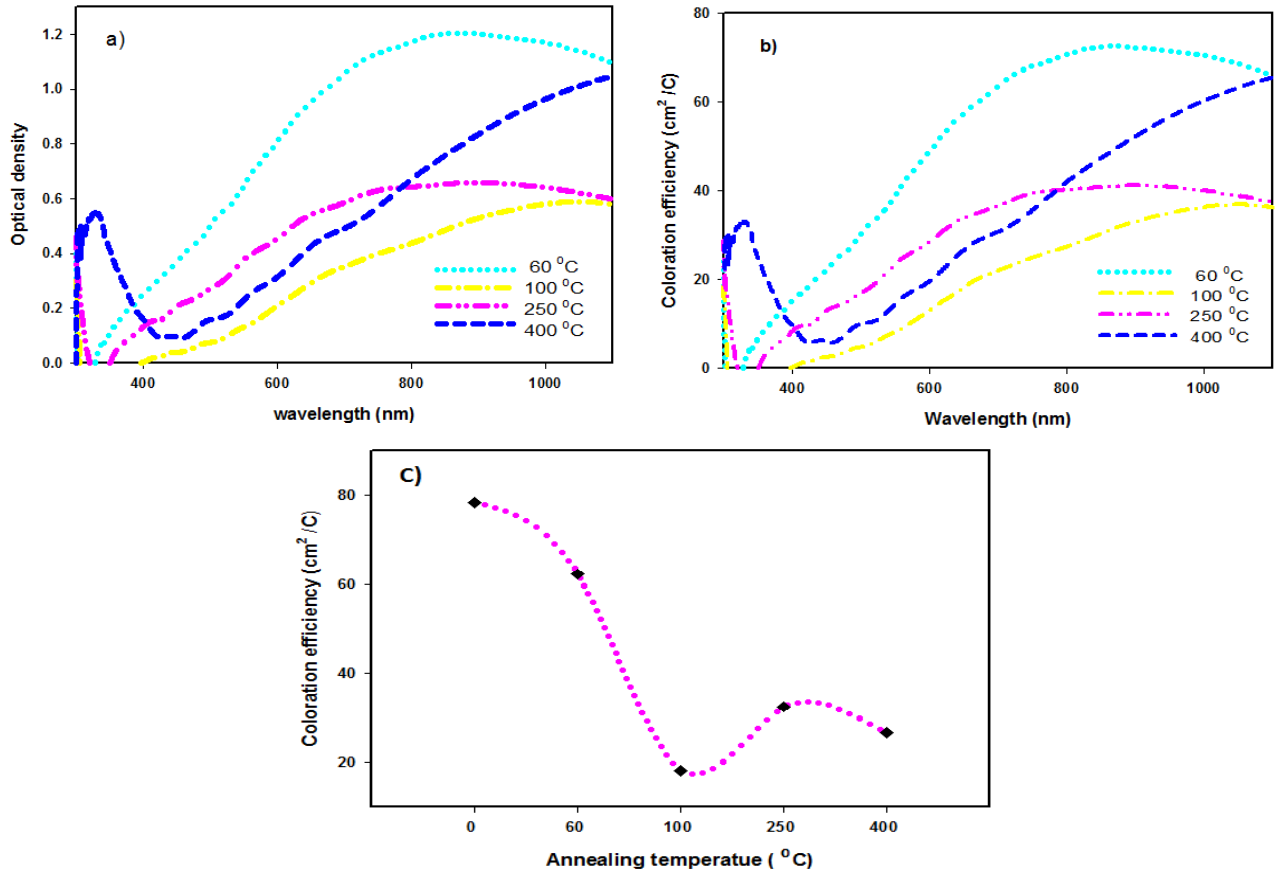

Figure 6. (a) optical density, (b) coloration efficiencies of WO_3 films annealed at 60°C, 100°C, 250 °C and 400 °C within $300 \leq \lambda \leq 1100$ nm range, (c) coloration efficiency of WO_3 with annealing temperature at λ=638 nm.

These figures show that the highest value of the coloration current was achieved for films while they were being deposited and the film which was annealed at 60°C. The highly porous structure of film when it was deposited and the film which was annealed at 60°C facilitates electrolyte penetrating into the particles and shortens the ions diffusion path within the bulk of tungsten oxide. Meanwhile, the intercrossing network provides many paths for double injection/extraction of ions and electrons to/ from the film. All these contribute to the improvement of optical and electrochromic performance. These properties make the film that was annealed at 60°C an interesting option in making efficient EC window. Films which were annealed at high temperatures yielded lower coloration currents because they have higher particles size and lower cracks. In addition, the overall area of a CV is a measure of the intercalated charge; thus, films that yield large CV areas are more suitable for electrochromic applications.

In figure 5 the area of CV decreases when annealing temperature increases. The decreased CV area observed in films as a result of rising annealing temperature can be attributed to reduction and narrowing of crack and large size particles, which decreases ion mobility of films. Both reduction and oxidation peaks of as-deposited films and annealed films at 60°C are significantly stronger than annealed films at high temperatures. This reflects that both films have higher insertion/extraction capacity for electrons and ions while they are being deposited and annealed at 60°C. These films have maximum oxidation current (46.765 mA and 40.354 mA at -0.324 mV, respectively). They also exhibit two larger negative currents (colored)(-53.211 and -52.491 mA, respectively). It can be seen that by increasing voltage, the current raises steadily from negative value up to a maximum and then diminishes to zero, which corresponds to the coloration of the film. This process is attributed to the following reversible electrochemical reaction:

$$WO_3 + x\,Li^+ + xe^- \rightarrow Li_xWO_3 . \quad (3)$$

The amount of Li+ intercalated/deintercalated) into/ out of the films, which can be estimated from CVs, decreases by increasing the annealing temperature. This is because of the growth of crystallinity of films during annealing and also the shrink of crack for Li ion intercalation and deintercalation.

Electrochromic performance mostly depends on the following parameters. Coloration Efficiency is a very important parameter that was calculated by changing optical density with charges intercalated per unit electrode area. The change in optical density (ΔOD) and coloration efficiency were calculated using the following relations:

$$\Delta OD(\lambda) = \mathrm{Log}\left[T_{bleached}(\lambda)/T_{colored}(\lambda)\right], \quad (4)$$

$$CE(\lambda) = \eta = \Delta OD\,(\lambda)/Q, \quad (5)$$

where $T_{bleached}$ and $T_{colored}$ are the transmittance in the bleached and colored states respectively. Q is the

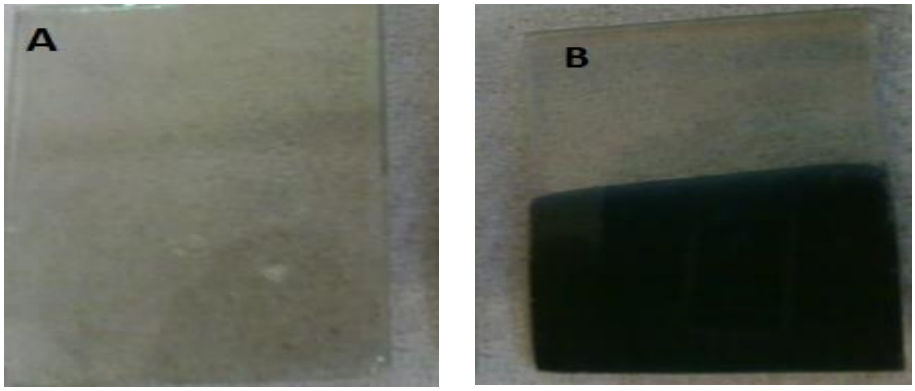

Figure 7. Transmittance change of WO_3 film annealed at 60 °C in a halfcell, (a) bleached state, (b) colored state.

intercalated charge density, which corresponds to the ratio of the inserted charge over the device area.

Figure. 6 shows the precise comparison of OD and CE in WO_3 films with different annealing temperatures. WO_3 film that is annealed at 60°C shows high OD or CE in the visible region; however, it presents relatively low ones in the NIR. A high value of *CE* indicates that the EC film exhibits large optical modulation with small charge inserted or extracted. The comparatively high *CE* is attributed to large cracks of the WO_3 film, which provides more surface area and direct paths for the process of Li^+ intercalation or deintercalation. Figure 2b illustrates the transmission modulation as a function of annealing temperature. This figure reveals maximum transmission modulation for WO_3 film, which is annealed at 60°C. In order to explore the electrochromic property in more details the result of figure 6b is quantified in figure 6c.

Coloration efficiency increases as a function of wavelength and acquires values greater than η_{VIS} = 64.1 $cm^2\ C^{-1}$ and η_{NIR} = 73.3 $cm^2\ C^{-1}$ for annealed film at 60°C. The relatively high W^{5+} content in this film is responsible for its large electrochromic efficiency. A coloration efficiency of 40 $cm^2\ C^{-1}$ (λ = 550 nm) was observed by Choy et al. [32] for a poly (acrylic acid) / WO_3 hybrid film under a fixed lithium intercalation level of 12.5 mC cm^{-2}. Ashrit [33] obtained an integrated transmission modulation of 45% over the visible region for vacuum evaporated WO_3 films with 12.5 mC cm^{-2} of charge. The coloration efficiency of WO_3 films which are electrodeposited at −0.65 V from a $Na_2WO_4 + H_2O_2$ sol was 66 $cm^2\ C^{-1}$ at 633 nm [34]. Brezesinski [35] observed an electrochromic efficiency of 40 $cm^2\ C^{-1}$ for WO_3 deposits that were colored in a lithium electrolyte. Our integrated values of coloring efficiency are comparable to those reported by others for WO_3 deposits that were prepared by wet chemical techniques. The coloring efficiency of the annealed films (λ = 700 nm) has been compared in figure 6. For the annealed film at 60 °C, a maximum efficiency 72.8 $cm^2\ C^{-1}$ is obtained at 842.3 nm and it drops to low values at 1100 nm. The annealed film at 100 °C and 250 °C shows slightly lower efficiency values and the annealed film at 400 °C exhibits the worst electrochromic behavior with η_{VIS} ~ 24.4 $cm^2\ C^{-1}$ in λ = 638 nm.

It is obvious that the film that was annealed at 60°C offers the best changes for transmission modulation, absorption in the colored state and coloration efficiency.

Figure 7. shows the electrochromic performance of the annealed film at 60 °C in a half cell test. The WO_3 film showed a high contrast ratio between the colored and bleached state. Although WO_3 film turned into a very uniform dark blue color when polarized cathodically, it became transparent when polarized anodically. These changes are shown in figure 7.

4. Conclusion

Electrodeposited method has been developed to prepare WO_3 thin films. The open structure of annealed film at 60°C results in high transmission modulation (ΔT~65.9%), and coloration efficiency (η= 64.1$cm^2\ C^{-1}$) at λ = 638 nm. Poor performance of the films, which were annealed at elevated temperatures is related to dense microstructure. Subsequent to cycling, the electrochemical reversibility for the redox processes involving the insertion and extraction of lithium ions is attained only for the annealed film at 60°C. This film also exhibited an excellent transmittance modulation effect on the visible light. The surface morphology of the films was investigated and the results indicated that the annealed film at 60°C for 90 min had remarkable reversible electrochromic properties and its electrochromic reversibility was also very good.

References

1. S Green, J Backholm, P Georen, C G Granqvist, and G A Niklasson, *Sol. Energy Mat. Sol. C* **93** (2009) 2050.
2. L Yang, D Ge, J Zhao, Y Ding, X Kong, and Y Li, *Sol. Energy Mat. Sol. C* **100** (2012) 251.
3. A E Aliev and H W Shin, *Displays* **23** (2002) 239.
4. C G Granqvist, P C Lansaker, N R Mlyuka, G A Niklasson, and E Avendano, *Sol. Energy Mat. Sol. C* **93** (2009) 2032.
5. S N Alamri, *Sol. Energy Mat. Sol. C* **93** (2009)1657.
6. R Baetens, B P Jelle, and A Gustavsen, *Sol. Energy Mat. Sol. C* **94** (2010) 87.

7. H Huang, J Tian , W K Zhang, Y P Gan, X Y Tao, X H Xia, and J P Tu, *Electrochim. Acta* **56** (2011) 4281.
8. C G Granqvist, S Green, G A Niklasson, N R Mlyuka, S von Kraemer, and P Georen, *Thin Solid Films* **518** (2010) 3046.
9. J Zhang, X L Wang, Y Lu, Y Qiao, X H Xia, and J P Tu, *J. Solid State Electr***. 15** (2011) 2213.
10. K Tajima, Y Yamada, S H Bao, M Okada, and K Yoshimura, *Vacuum* **84** (2010) 1460.
11. K Hari Krishna, O M Hussain, and C M Julien, *Appl. Phys. A* **99** (2010) 921.
12. B Baloukas, J M Lamarre, and L Martinu, *Sol. Energ. Mat. Sol. C* **95** (2011) 807.
13. X H Xia, J P Tu, J Zhang, X L Wang, W K Zhang, and H Huang, *ACS Appl. Mater. Interfaces* **2** (2010) 186.
14. B Yang, P R F Barnes, W Bertram, and V Luca, *J. Mater. Chem.* **17** (2007) 2722.
15. M Deepa, A K Srivastava, S N Sharma, G Govind, and S M Shivaprasad, *Appl. Surf. Sci*. **254** (2008) 2342.
16. M Giannouli and G Leftheriotis, *Sol. Energy Mat. Sol. C* **95** (2011) 1932.
17. A H Yan, C S Xie, D W Zeng, S Z Cai, and H Y Li, *J. Alloys Compd.* **495** (2010) 88.
18. J Zhang, X L Wang, X H Xia, C D Gu, Z J Zhao, and J P Tu, *Electrochim. Acta* **55** (2010) 6953.
19. R Deshpande, S H Lee, A H Mahan, P A Parilla, K M Jones, A G Norman, B To, J L Blackburn, S Mitra, and A C Dillon, *Solid State Ion.* **178** (2007) 895.
20. H S Shim, J W Kim, Y E Sung, and W B Kim, *Sol. Energy Mat. Sol. C* **93** (2009) 2062.
21. B B Cao, J J Chen, X J Tang, and W L Zhou, *J. Mater. Chem.* **19** (2009) 2323.
22. J Zhang, X L Wang, X H Xia, C D Gu, and J P Tu, *Sol. Energy Mat. Sol. C* **95** (2011) 2107.
23. Y S Lin, S S Wu, and T H Tsai, *Sol. Energ. Mat. Sol. C* **94** (2010) 2283.
24. W Cheng, E Baudrin, B Dunn, and J I Zink, *J. Mater. Chem*. **11** (2001) 92.
25. S Badilescu and P V Ashrit, *Solid State Ionics* **158** (2003) 187.
26. N Ozer, *Thin Solid Films* **304** (1997) 310.
27. P K Biswas, N C Pramanik, M K Mahapatra, and D Ganguli, *J. Livage, Mater. Let*. **57** (2003) 4429.
28. I Shiyanovskaya, M Hepel, and E Tewksburry, *J. New Mat. Elect. Syst.* **3** (2000) 241.
29. H Yang, F Shang, L Gao, and H Han, *Appl. Surf. Sci.* **253** (2007) 5553.
30. M Regragui, M Addou, B El Idrissi, J C Bernede, A Outzourhit, and E Ec chamikh, *Mater. Chem. Phys.* **70** (2001) 84.
31. M Deepa, R Sharma, A Basu, and S A Agnihotry, *Electrochim. Acta* **50** (2005) 3545.
32. J H Choy, Y I Kim, B W Kim, N G Park, G Campet, and J D Grenier, *Chem. Mater*. **12** (2000) 2950.
33. P V Ashrit, *Thin Solid Films* **385** (2001) 81.
34. T Pauporte, *J. Electrochem. Soc.* **149** (2002) C539.
35. T Brezesinki, D F Rohlfing, S Sallard, M Antonietti, and B M Smarsly, *Small* **2** (2006) 1203.